Functional Materials 19, No.3 (2012) 

# Radiation induced defects in $M_{1-x}Pr_xF_{2+x}$ ($M^{2+}$ = Ca, Sr, Ba, $x = 0.35$) solid solutions

*I.A.Boiaryntseva, N.V.Shiran, A.V.Gektin*

Institute for Scintillation Materials, STC "Institute for Single Crystals" National Academy of Sciences of Ukraine, 60 Lenin Ave., 61001 Kharkiv, Ukraine

*Received July 4, 2012*

Radiation-induced processes in $M_{1-x}Pr_xF_{2+x}$ ($M^{2+}$ = Ca, Sr, Ba, $x = 0.35$) solid solutions have been studied. It is shown that the radiation coloration of $M_{0.65}Pr_{0.35}F_{235}$ crystals is due to the trapping of charge carriers at anion sublattice defects. The efficiency of color centers formation in the investigated solid solutions grows in the row Ca → Sr → Ba. It may be caused by the increase of the pre-irradiation defects as a result of the different cluster types formation in $M_{0.65}Pr_{0.35}F_{2.35}$ mixed systems.

Исследованы радиационно-стимулированные процессы в твердых растворах $M_{1-x}Pr_xF_{2+x}$ ($M^{2+}$ = Ca, Sr, Ba, $x = 0.35$). Показано, что радиационное окрашивание кристаллов $M_{0,65}Pr_{0.35}F_{2.35}$ может быть обусловлено захватом носителей заряда на дефектах анионной подрешетки. Эффективность образования центров окраски в кристаллах $M_{0.65}Pr_{0.35}F_{2.35}$ увеличивается в ряду Ca → Sr → Ba. Последнее может быть связано с ростом количества дорадиационных дефектов за счет образования различных типов кластеров в системах $M_{0.65}Pr_{0.35}F_{2.35}$.

## *1. Introduction*

Nonstoichiometric fluorite-structured $M_{1-x}R_xF_{2+x}$ ($M^{2+}$ = Ca, Sr, Ba, $R^{3+}$ = Ln, $x \le 0.5$) solid solutions give an opportunity to modify the material properties through variation of composition and defect structure. Luminescent study of these crystals in case of $R^{3+}$ = Ce, Eu, Pr points to the essential changes in their parameters as compared with low doped $MF_2$:R crystals [1–4].

Since the mixed crystals correspond to multi-component systems, their radiation stability should be depended on types of $M^{2+}$ and $R^{3+}$ ions and $RF_3$ concentration. The first results of investigations on radiation stability of $M_{1-x}R_xF_{2+x}$ solid solutions were presented in [5, 6]. The study of $Ba_{1-x}R_xF_{2+x}$ (R = $La^{3+}$, $Ce^{3+}$, $0.01 \le x \le 0.45$) crystals revealed the complex dependence of radiation coloration on $RF_3$ content [4, 7]. High radiation stability was found for $Ca_{0.65}Eu_{0.35}F_{2.35}$ and $M_{0.65}Ce_{0.35}F_{2.35}$ (M = Ca, Sr, Ba) crystals [1, 2].

The present work is devoted to investigation of radiation-induced phenomena in high-concentrated $M_{1-x}Pr_xF_{2+x}$ ($M^{2+}$ = Ca, Sr, Ba, $x$ = 0.35) solid solutions.

## *2. Experimental*

Mixed crystals $M_{0.65}Pr_{0.35}F_{2.35}$ were grown from high purity (>99.99 %) powders by the Bridgman technique in $CF_4$ atmosphere [8]. Chemical composition of the solid solutions determined by electron probe microanalysis (EPMA) and inductively coupled plasma atomic emission spectroscopy (ICP-AES) corresponds to $M_{0.65}Pr_{0.35}F_{2.35}$.

According to XRD analysis $M_{0.65}Pr_{0.35}F_{2.35}$ crystals have fluorite lattice and do not contain $PrF_3$ phase. A partial deficiency in the main fluorine positions (anion vacancies) as

well as excessive interstitial fluorine ions was revealed in these mixed compounds.

The crystals were X-ray irradiated (W-anode, 160 kV, 9 mA) at room temperature. Absorption spectra were recorded by SPECORD 40 spectrophotometer. Thermally stimulated luminescence measurements were performed with the heating rate of 0.2°C/s. Emitted light was registered by PMT-100. Afterglow spectra were recorded using FLS 920 Edinburgh Instruments spectrometer.

### 3. Results

X-ray irradiation of $M_{0.65}Pr_{0.35}F_{2.35}$ (M = Ca, Sr, Ba) crystals at 300 K results in the appearance of additional absorption in UV and VIS spectral ranges (Fig. 1). The number of strongly overlapping bands does not allow their separation and identification. Absorption in 200–260 nm range are expected to be due to hole-type centers [9]. The bands with maxima around 310–330 nm are traditionally assigned to hole centers stabilized by rare-earth ion [10, 11]. In the longer wavelength range the bands at ~ 370–390, 425 and ~500 nm are revealed for $Ca_{0.65}Pr_{0.35}F_{2.35}$, $Sr_{0.65}Pr_{0.35}F_{2.35}$ and $Ba_{0.65}Pr_{0.35}F_{2.35}$ crystals, respectively. Their positions are typical for *F*-type absorption bands in alkali-earth fluoride crystals $CaF_2$, $SrF_2$ and $BaF_2$ [12–14].

Integral of the induced absorption spectra plotted against the irradiation time for $M_{0.65}Pr_{0.35}F_{2.35}$ crystals are presented in Fig. 2a. It is clearly seen the linear grows of the induced absorption with dose without saturation up to $D \approx 120$ Gy. This fact implies the high concentration of pre-radiation defects. The coloration efficiency (evaluated as an integral of the induced absorption)

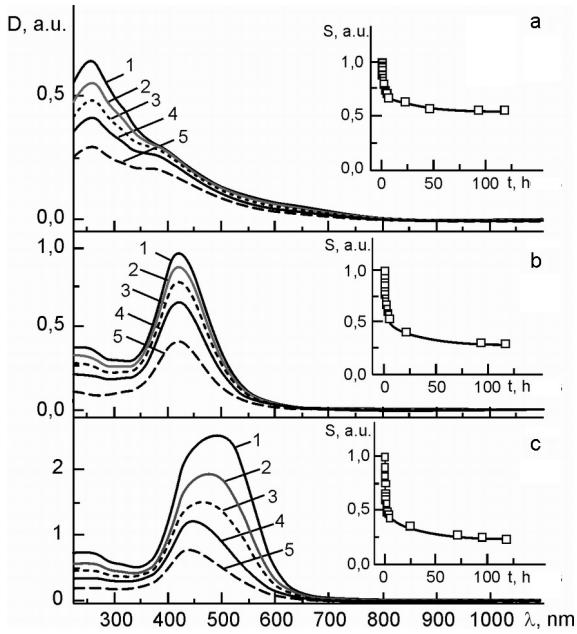


Fig. 1. Induced absorption spectra of $Ca_{0.65}Pr_{0.35}F_{2.35}$ (a), $Sr_{0.65}Pr_{0.35}F_{2.35}$ (b), $Ba_{0.65}Pr_{0.35}F_{2.35}$ (c) crystals recorded in 5 min. (*1*), 20 min. (*2*), 60 min. (*3*), 4 h. (*4*), 5 days (*5*) after X-irradiation. Inset: annealing of color centers (integral under the induced absorption curve) at 300 K. Dose 80 Gy.

increases in the row $Ca \rightarrow Sr \rightarrow Ba$, as shown in Fig. 2b.

General decrease of the induced absorption starts immediately after irradition. In the case of $Ba_{0.65}Pr_{0.35}F_{2.35}$ the color centers destruction is accompanied by shift of the band from ~500 to 450 nm. The latter reveals the presence of several types of induced centers.

The bleaching process comes about stage-by-stage which is indicative of the different

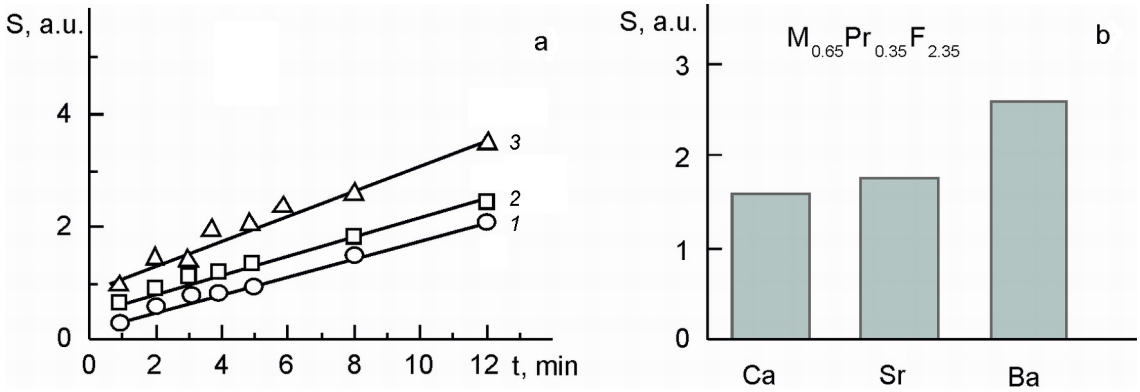


Fig. 2. Integral of the induced absorption spectra vs. irradiation time for $Ca_{0.65}Pr_{0.35}F_{2.35}$ (*1*), $Sr_{0.65}Pr_{0.35}F_{2.35}$ (*2*), $Ba_{0.65}Pr_{0.35}F_{2.35}$ (*3*) (a). Dose rate ~10 Gy/min. Coloration efficiency of $M_{0.65}Pr_{0.35}F_{2.35}$ crystals irradiated by dose 80 Gy (b).

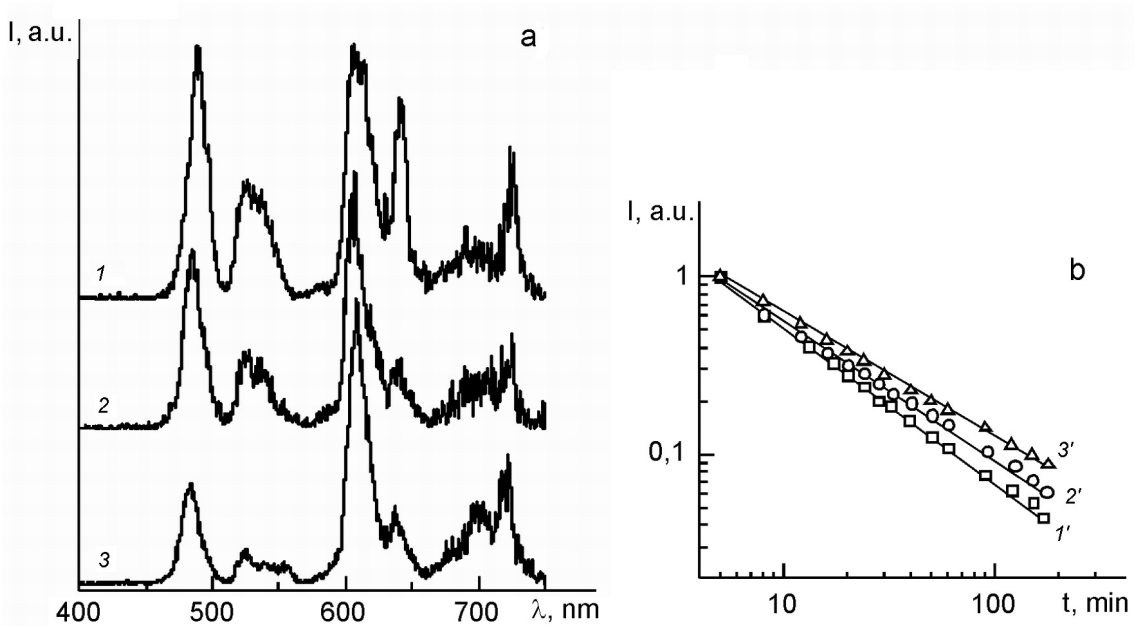


Fig. 3. Afterglow spectra (a) and decay (b) in X-irradiated $Ca_{0.65}Pr_{0.35}F_{2.35}$ (*1*, *1′*), $Sr_{0.65}Pr_{0.35}F_{2.35}$ (*2*, *2′*) and $Ba_{0.65}Pr_{0.35}F_{2.35}$ (*3*, *3′*) crystals. $D$ = 80 Gy, 300 K.

thermal stability of induced defects (see insets in Fig. 1). The initial fast stage with duration of about 4–5 h. is accounted of centers unstable at room temperature, whereas the presence of the second, slow stage indicates the presence of deeper traps. The first stage of the color centers destruction is accompanied by the afterglow corresponded to $^3P_0 \rightarrow 4f^2$ radiative transitions in $Pr^{3+}$ ion (Fig. 3a). Afterglow decay follows a hyperbolic low $I \sim t^{-p}$ where $p$ is less than 1 (0.85, 0.75 and 0.68 for $Ca_{0.65}Pr_{0.35}F_{2.35}$, $Sr_{0.65}Pr_{0.35}F_{2.35}$, $Ba_{0.65}Pr_{0.35}F_{2.35}$, respectively) (Fig. 3b) which is typical for tunnelling mechanism of recombination processes [15].

Thermostimulated luminescence (TSL) of the crystals irradiated at 300 K is shown in Fig. 4. Peaks at ~50°C ($Ca_{0.65}Pr_{0.35}F_{2.35}$), ~80°C ($Sr_{0.65}Pr_{0.35}F_{2.35}$) and ~75°C ($Ba_{0.65}Pr_{0.35}F_{2.35}$) are present in the low-temperature range. These peaks are responsible for observed afterglow and the first stage of induced absorption relaxation. The series of high-temperature peaks at ~115, 175, 330°C ($Ca_{0.65}Pr_{0.35}F_{2.35}$), ~230°C ($Sr_{0.65}Pr_{0.35}F_{2.35}$) and ~105, 175, 290, 400°C ($Ba_{0.65}Pr_{0.35}F_{2.35}$) correlates with the presence of the second, slow stage of color centers destruction.

It should be noted that extremely low TSL intensity of $M_{0.65}Pr_{0.35}F_{2.35}$ crystals complicates the study of the recombination spectra. For qualitative analysis of emission in TSL peaks filters with different transmission were used (see Fig. 4d). The spectral composition of TSL peaks in 50–150°C region for all $M_{0.65}Pr_{0.35}F_{2.35}$ samples corresponds to $\lambda > 450$ nm range and can be ascribed to $^3P_0 \rightarrow 4f^2$ radiative transitions in $Pr^{3+}$ ions which were observed in afterglow spectra at room temperature.

On the contrary, emission in high-temperature peaks belongs to UV region ~280–380 nm. Luminescence in the most prominent peak at 175°C in $Ba_{0.65}Pr_{0.35}F_{2.35}$ corresponds to radiative transitions in $Ce^{3+}$ ions. Emission intensities for the rest of the high-temperature peaks are lower than sensitivity of the experimental set-up. The same situation takes place in $Ca_{0.65}Pr_{0.35}F_{2.35}$ and $Sr_{0.65}Pr_{0.35}F_{2.35}$ crystals.

It should be noted that presence of $Ce^{3+}$ ions are revealed in emission spectra under photo- and X-ray excitation. Concentration of $Ce^{3+}$ ions in $M_{0.65}Pr_{0.35}F_{2.35}$ crystals grows in the row Ca → Sr → Ba. Based on this fact one can suppose high temperature TSL peaks are due to recombination of charge carriers on $Ce^{3+}$ ions.

## *4. Discussion*

When analizing radiation-induced effects in high-concentrated solid solutions one should take into account their structural properties. $M_{1-x}R_xF_{2+x}$ (M = Ca, Sr, Ba, $x \leq 0.5$) mixed systems have fluorite lattice

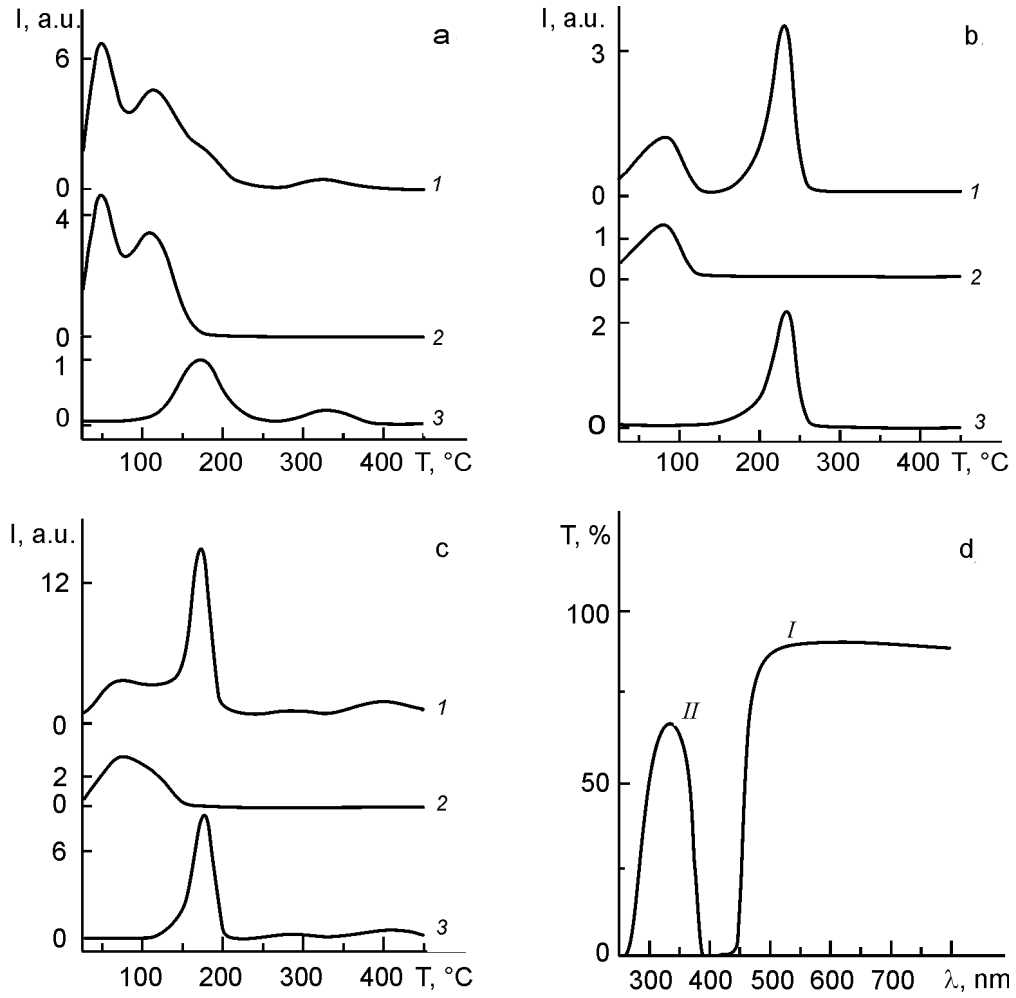


Fig. 4. TSL glow curves of $Ca_{0.65}Pr_{0.35}F_{2.35}$ (a), $Sr_{0.65}Pr_{0.35}F_{2.35}$ (b), $Ba_{0.65}Pr_{0.35}F_{2.35}$ (c) measured without filter (*1*) and using filter I (*2*), II (*3*). $D$ = 80 Gy, 300 K. Transmittance of the filters (d).

and contain an excess of anion vacancies ($\upsilon_a^+$) and interstitial fluorine ions ($F_i^-$) [16–18]. Typical feature of the nonstoichiometric solid solutions is the formation of defect clusters which include alkali-earth $M^{2+}$ and rare-earth $R^{3+}$ ions as well as $\upsilon_a^+$ and $F_i^-$.

Composition and structure of the clusters depend on the ratio of the ionic radii ($r$) of rare-earth ($R^{3+}$) and the host ($M^{2+}$) cations $r(R^{3+})/r(M^{2+})$ [16]. If this relation is close to 1.02–1.08 the formation of $[(M,R)_4F_{26}]$ clusters takes place. Besides $M^{2+}$ and $R^{3+}$ ions this type of clusters includes one anion vacancy and three (or four) fluorine interstitials $F_i^-$. When $r(R^{3+})/r(M^{2+}) \approx 0.7$–$0.8$, $[(M,R)_6F_{36}]$ clusters, containing up to eight anion vacancies and twelve interstitial fluorine ions, are typical. Schematic view of the possible cluster types is shown in Fig. 5.

In $M_{0.65}Pr_{0.35}F_{2.35}$ systems $r(Pr^{3+})/r(M^{2+})$ ratio equals 1.07, 0.95 and 0.79 for $Ca_{0.65}Pr_{0.35}F_{2.35}$, $Sr_{0.65}Pr_{0.35}F_{2.35}$ and $Ba_{0.65}Pr_{0.35}F_{2.35}$, respectively (values of ionic radii are taken from [16, 19]). For $Ca_{0.65}Pr_{0.35}F_{2.35}$ crystals one can suppose the formation of $[(M,R)_4F_{26}]$ clusters whereas for $Ba_{0.65}Pr_{0.35}F_{2.35}$ system $[(M,R)_6F_{36}]$ clusters should be typical. In the case of $Sr_{0.65}Pr_{0.35}F_{2.35}$ the presence of both cluster types are expected.

The specificity of $M_{1-x}Pr_xF_{2+x}$ solid solutions is the great number of preirradiation defects — $\upsilon_a^+$ and $F_i^-$ which may capture electrons and holes created under X-irradiation. The presence of the bands attributed to $F$- and $V$-type color centers in induced absorption spectra confirms this assumption. Taking into account different clusters types in $M_{0.65}Pr_{0.35}F_{2.35}$ crystals the concentration of pre-irradiation defects should increase in Ca → Sr → Ba row. This fact explains the experimentally observed growth of coloration efficiency of mixed systems in sequence of

$Ca_{0.65}Pr_{0.35}F_{2.35} \rightarrow$ $Sr_{0.65}Pr_{0.35}F_{2.35} \rightarrow$ $Ba_{0.65}Pr_{0.35}F_{2.35}$.

Afterglow decay of $M_{0.65}Pr_{0.35}F_{2.35}$ solid solutions points to a tunnelling recombination. The main condition for tunnelling processes is overlapping of wave-functions of recombination centers, i.e. small distance between defects. Mixed systems are expected to satisfy this condition since the most part of possible traps are concentrated in the clusters. Tunnelling recombination also may be thermally assisted [20, 21]. The observation of low-temperature TSL peaks for $x$-irradiated $M_{0.65}Pr_{0.35}F_{2.35}$ crystals (see Fig. 4) allows us to suggest the thermally assisted tunnelling processes in the mixed systems.

In this case the energy of thermally assisted tunnelling recombination of electrons and holes at lattice defects may be non-radiatively transferred to $^3P_0$ level of $Pr^{3+}$ ions. The following $^3P_0 \rightarrow 4f^2$ radiatively transitions are observed in afterglow. It should be noted that $4f^15d^1 \rightarrow 4f^2$ and $^1S_0 \rightarrow 4f^2$ luminescence of $Pr^{3+}$ ions observed under photo- and X-ray excitation are absent in the afterglow spectra. The energy of charge carriers recombination may be enough for excitation of $^3P_0$ level but too small for population of high-energy $4f^15d^1$ (~5.5–5.6 eV) and $^1S_0$ (~5.8 eV) states of $Pr^{3+}$ ions.

High-temperature TSL peaks in $M_{0.65}Pr_{0.35}F_{2.35}$ crystals correspond to luminescence of $Ce^{3+}$ ions which are present in mixed systems as uncontrolled impurities. The recombination of electrons and holes in this case may take place via delocalized states with the following excitation of $5d$ levels of $Ce^{3+}$. Due to high radiative efficiency $5d \rightarrow 4f$ transitions in $Ce^{3+}$ may be observed in TSL spectra even at trace cerium impurity in crystals.

Absorption bands typical for transitions in divalent $Pr^{2+}$ ions in alkali-earth fluoride crystals [22, 23] have not been revealed in irradiated $M_{0.65}Pr_{0.35}F_{2.35}$ crystals. The similar effect of reduced efficiency for radiation-induced reaction $R^{3+} + e^- \rightarrow R^{2+}$ with the increase in $R^{3+}$ content was observed for $M_{1-x}R_xF_{2+x}$ systems in [5]. According to [22–25] only single $Pr^{3+}$ ions in cubic, tetragonal or trigonal sites can be reduced by irradiation in alkali-earth fluoride crystals. In the mixed systems the concentration of such sites are expected to be low since the most part of praseodymium ions are concentrated in clusters. So, the contribution of this charge conversion process to radiation coloration of $M_{0.65}Pr_{0.35}F_{2.35}$ solid solutions should be negligible. Besides, a competition for electron trapping between $Pr^{3+}$ ions and anion defects may occur in $M_{0.65}Pr_{0.35}F_{2.35}$ systems.

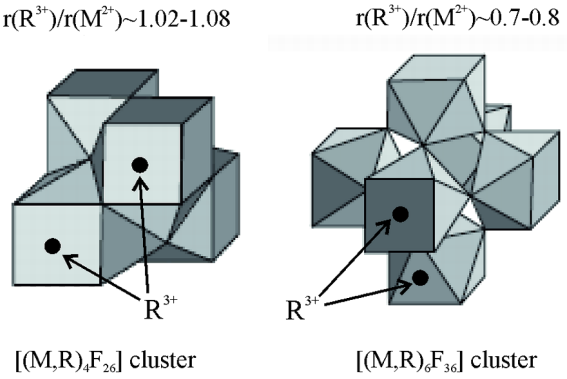


Fig. 5. Schematic view of the possible cluster types in $M_{0.65}Pr_{0.35}F_{2.35}$ crystals [17].

At the same time in rare-earth doped $MF_2$ crystals $R^{3+}$ ions can trap holes [26, 27]. According to [27] the efficiency of $R^{3+}$ conversion into tetravalent state as the result of oxidation reaction $R^{3+} + h \rightarrow R^{4+}$ tends to grow with increase in $R^{3+}$ concentration. The presence of $Pr^{4+}$ ions in X-irradiated at 300 K $Cs_2NaYF_6$:Pr crystals was revealed by EPR technique in [28]. However experimental data as to absorption of $Pr^{4+}$ in UV-VIS spectral ranges for fluoride hosts are absent. One can only suppose the hole trapping at $Pr^{3+}$ and impurity $Ce^{3+}$ ions in $M_{0.65}Pr_{0.35}F_{2.35}$ mixed systems. In this case anion vacancies serve as electron traps. However the possibility of this mechanism requires additional extensive studies.

## 5. Conclusions

Radiation-induced phenomena in $M_{0.65}Pr_{0.35}F_{2.35}$ ($M^{2+}$ = Ca, Sr, Ba) have been studied. The data obtained indicate that the color centers creation in $M_{0.65}Pr_{0.35}F_{2.35}$ crystals is due to the trapping of charge carriers at anion sublattice defects. The coloration efficiency of the investigated solid solutions grows in Ca → Sr → Ba row. This result is in line with the suggested increase in the concentration of pre-irradiation defects in $Ca_{0.65}Pr_{0.35}F_{2.35} \rightarrow$ $Sr_{0.65}Pr_{0.35}F_{2.35} \rightarrow$ $Ba_{0.65}Pr_{0.35}F_{2.35}$ sequence due to occurrence of different cluster types. The following destruction of radiation-induced defects may occur via thermally assisted tunnelling recombination of charge carriers.

Contrary to low doped $MF_2$:Pr crystals, absorption bands typical to transitions in

$Pr^{2+}$ were not found in X-ray induced absorption spectra of $M_{0.65}Pr_{0.35}F_{2.35}$ crystals. Taking into account the structural properties of the mixed systems this fact may be explained by negligible concentration of single $Pr^{3+}$ ions which can be reduced by irradiation.

The authors are grateful to Dr.V.N.Baumer (SSI "Institute for Single Crystals" NASU) and Dr.K.Shimamura (National Institute for Materials Science, Japan).

This work is supported by 7th FP INCO.2010-6.1 grant agreement No. 266531 (project acronym SUCCESS).

### *References*

1. A.Gektin, N.Shiran, V.Nesterkina et al., *IEEE Tras. Nucl. Sci*, **56**, 1002 (2009).
2. A.Gektin, N.Shiran, V.Nesterkina et al., in: Proc. Int. Conf. on Inorg. Scintillators and Their Application SCINT' 2005, Alushta, Ukraine (2005), p.419.
3. A.Gektin, N.Shiran, V.Nesterkina et al., *J. Luminescence*, **130**, 2277 (2010).
4. M.Kobayashi, M.Ishii, B.P.Sobolev et al., *Nucl. Instr. Meth. Phys. Res. A*, **421**, 191 (1999).
5. Y.Rustamov, G.A.Tavshunsky, P.K.Habibulaev et al., *Zh. Tekhn. Fiz.*, **55**, 1150 (1985).
6. Sh.A.Vahidov, G.A.Tavshunsky, Y.Rustamov et al., *Zh. Tekhn. Fiz.*, **49**, 1943 (1979).
7. E.A.Radzhabov, A.Shalaev, A.I.Nepomnyashikh, *Rad.Meas.*, **29**, 307 (1998).
8. K.Shimamura, E.Villora, S.Nakakita et al., *J. Cryst. Growth*, **264**, 208 (2004).
9. V.A.Arhangelskaya, B.I.Maksakov, P.P.Feofilov, *Fiz.Tverd.Tela*, **7**, 2260 (1965).
10. P.V.Figura, A.I.Nepomnyashikh, E.A.Radzhabov, *Optika i Spektroskopiya*, **67**, 1304 (1989).
11. J.H.Beaumont, W.Hayes, D.L.Kirk et al., *Proc.Roy.Lond.A*, **315**, 69 (1970).
12. J.H.Beaumont, W.Hayes, *Proc.Roy.Soc.A*, **309**, 41 (1969).
13. B.C.Cavenett, W.Hayes, I.C.Hunter et al., *Proc.Roy.Soc.A*, **309**, 53 (1969).
14. A.I.Nepomnyashikh, E.A.Radzhabov, A.V.Egranov et al., *Rad.Eff.and Def.in Solids*, **157**, 715 (2002).
15. V.V.Pologrudov, I.V.Grigorov, *Fiz.Tverd. Tela*, **46**, 1781 (2004).
16. L.A.Muradyan, B.A.Maksimov, V.I.Simonov, *Koordinatsionnaya Chim.*, **12**, 1398 (1986).
17. B.P.Sobolev, A.M.Golubev, P.Herrero, *Crystallography Rep.*, **48**, 141 (2003).
18. J.P.Laval, A.Abaouz, B.Frit, *J.Solid State Chem.*, **81**, 271 (1989).
19. L.H.Ahrens, *Geochim.et Cosmochim.Acta*, **2**, 155 (1952).
20. S.W.S.McKeever, Thermoluminescence of Solids, Cambridge University Press (1985).
21. A.Vedda, M.Martini et al., *Phys.Rev.B*, **61**, 8081 (2000).
22. D.S.McClure, Z.Kiss, *J.Chem.Phys.*, **39**, 3251 (1963).
23. J.L.Merz, P.S.Pershan, *Phys.Rev.*, **162**, 217 (1967).
24. S.H.Batygov, V.V.Osiko, *Fiz.Tverd.Tela*, **13**, 2247 (1971).
25. L.S.Kornienko, A.O.Rybaltovskiy, Spektroskopiya Kristallov, Nauka, Moscow (1975) [in Russian].
26. S.H.Batygov, Yu.K.Voron'ko, *Neorganicheskie Materialy*, **5**, 1048 (1969).
27. S.H.Batygov, R.G.Mikaelyan, V.V.Osiko et al., *Neorgan. Mater.*, **3**, 760 (1967).
28. Th.Pawlik, J.M.Spaeth, *J.Appl.Phys.*, **82**, 4236 (1997).

## Радіаційні дефекти у твердих розчинах $M_{1-x}Pr_xF_{2+x}$ ($M^{2+}$ = Ca, Sr, Ba, $x = 0.35$)

***Я.А.Бояринцева, Н.В.Ширан, О.В.Гектін***

Досліджено радіаційно-стимульовані процеси у твердих розчинах $M_{1-x}Pr_xF_{2+x}$ ($M^{2+}$ = Ca, Sr, Ba, $x = 0.35$). Показано, що радіаційне забарвлення кристалів $M_{0.65}Pr_{0.35}F_{2.35}$ може бути зумовлено захопленням носіїв заряду на дефектах аніонної підгратки. Ефективність утворення центрів забарвлення в кристалах $M_{0.65}Pr_{0.35}F_{2.35}$ зростає в ряду Ca → Sr → Ba. Останнє може бути пов'язано зі збільшенням кількості дорадіаційних дефектів за рахунок утворення різних типів кластерів у системах $M_{0.65}Pr_{0.35}F_{2.35}$.